NJC

# Alkaline earth ion exchange study in pure silica LTA zeolites using periodic first-principles calculations



| | |
|---|---|
| Journal: | *New Journal of Chemistry* |
| Manuscript ID | NJ-ART-08-2019-004091.R1 |
| Article Type: | Paper |
| Date Submitted by the Author: | 25-Sep-2019 |
| Complete List of Authors: | Kocevski, Vancho; University of South Carolina, Nuclear Engineering Program<br>Hu, Shenyang; Pacific Northwest National Laboratory, Energy and Environment Directorate<br>Besmann, Theodore; University of South Carolina, Nuclear Engineering Program |
| | |

ARTICLE

# Alkaline earth ion exchange study in pure silica LTA zeolites using periodic first-principles calculations

Received 00th January 20xx,
Accepted 00th January 20xx

DOI: 10.1039/x0xx00000x

Vancho Kocevski,*[a,c] Shenyang Y. Hu [b,c] and Theodore M. Besmann [a,c]

Experiments show that Zeolites, such as Linde Type A (LTA), are promising materials for radioactive decontamination processes. In this work, the thermodynamic properties associated with alkaline earth ion ($Ca^{2+}$, $Sr^{2+}$ and $Ba^{2+}$) exchange in pure silica LTA was studied using periodic first-principles calculations. The adsorption energies of alkaline earth ions compared with that of $Na^{+}$ were investigated. The driving force for the alkaline earth exchange and related isotherms were calculated, and analyzed as a function of the electron chemical potential. The results demonstrate that $Na^{+}$ in a pure silica LTA can completely be removed by $Ba^{2+}$ and almost completely be removed by $Sr^{2+}$ from a stream, but cannot be effectively exchanged by $Ca^{2+}$. We also showed that electron-donating dopants should suppress the $Sr^{2+}$ and $Ba^{2+}$ ion exchange, and that there is a substantial preference for incorporating $Ba^{2+}$ over $Sr^{2+}$. Lastly, the substantial difference between the adsorption energies of the ions in an assumed vacuum and those computed in water suggests that a solvation model is needed for accurate representation of ion adsorption in an LTA zeolite.

## Introduction

Zeolites are naturally occurring or synthetic microporous aluminosilicate solids, with a hierarchical structure and a range of topologies. Their structural framework is composed of $MO_4$ corner-sharing tetrahedra (M = Si, Al), with varying arrangements. This allows for the tailoring of their pore and cage sizes to meet specific needs. Zeolites have distinct characteristics such as high specific surface area, surface acidity or basicity, uniform microporous structure, hydrothermal stability, and hydrophobicity. These properties make zeolites very versatile materials useful in a variety of industries as molecular sieves, catalysts, adsorbents, and selective ion exchange media [1,2,3,4,5,6,7,8,9,10, 11, 12]. Zeolites are currently also used for nuclear wastewater processing, mainly because they can easily retain many of the radionuclides. Once a zeolite has removed a contaminant, it can be processed into a ceramic waste form, permanently trapping radioactive elements and allowing for safe storage of the radioactive waste.

Recently, the Linde Type A (LTA) zeolite has garnered attention due to its capability for substantially exchanging $Na^{+}$ with other cations, demonstrating the highest exchange capacity feasible in zeolites, 5.4 meq/g [13]. This superior level of ion exchange has driven its use in diverse applications from enhancing detergent efficiency [14] and sorbents [15], and desalination [16] and treatment of wastewater [17,18,19]. LTA zeolites have also been considered for removing radionuclides such as $Cs^{+}$ and $Sr^{2+}$ from radioactive effluents [19,20,21]. In addition to numerous experimental studies, there is an increasing interest in modeling that complement the experimental findings or predict new/additional applications. However, the large size of the LTA zeolite has so far discouraged detailed modeling studies and only few have thus been carried out [22,23,24,25]. To explore useful modeling approaches, we used periodic first-principles calculations to investigate alkaline earth (AE) ion exchange in LTA zeolites.

In this effort we demonstrated capability of an LTA zeolite to sequester radionuclides from wastewater by analyzing $Na^{+}$ ion exchange with AE ions $Ca^{2+}$, $Sr^{2+}$ and $Ba^{2+}$ using first-principles calculations. To investigate the influence of the environment, AE ion adsorption and exchange were studied assuming vacuum or water surroundings, utilizing an implicit solvation model. The performance of Perdew, Burke and Ernzerhof (PBE) potential and Van der Waals corrections in estimating ion adsorption and exchange energies was also investigated. In addition, we analyzed the ion exchange probability as a function of the electron chemical potential, providing insight into how defects or environment, such as pH level, can influence ion exchange. Lastly, competing $Sr^{2+}$ and $Ba^{2+}$ ion exchange was analyzed, providing critical information on the probability of retaining these two competing radionuclides in LTA zeolite.

## Models and Methodology

The studied LTA zeolite is an aluminosilicate with the formula $Na_{12}[(AlO_2)_{12}(SiO_2)_{12}]\cdot xH_2O$ that contains a large amount of adsorption (exchange) sites. Its cubic framework is comprised of $\alpha$–cages (supercages), formed by 3D interconnected $\beta$–cages (sodalite cages) by double four-member rings (see red shaded area in Fig. 1). The pore system in the LTA zeolite is formed by the 8-membered apertures (site 3 in Fig. 1) that interconnect the $\alpha$–cages. The LTA zeolite has three unique adsorption sites, termed site 1, 2 and 3 with diameters of 4.4 Å, 3.6 Å and 6.9 Å, respectively (Fig. 1). Because of the large unit cell of 640 atoms, first-principles calculations are prohibitively expensive and thus we used pure silica LTA zeolite (ps-LTA zeolite), which has 72 atoms, as a model system. Ps-LTA zeolite has been synthesized using an organic structure-directing agent

[a] Nuclear Engineering Program, University of South Carolina, Columbia, 29208, USA
[b] Pacific Northwest National Laboratory, PO Box 999, Richland, WA 99352, USA
[c] Center for Hierarchical Wasteform Materials (CHWM), University of South Carolina, Columbia, SC, 29208 USA
* Corresponding author: kocevski@mailbox.sc.edu; vancho.vk@gmail.com
Electronic Supplementary Information (ESI) available: the ion's activity coefficient, and chemical potentials, dependence of the ion exchange energy of ion concentration ratio and electron chemical potential. See DOI: 10.1039/x0xx00000x

obtained by self-assembly [3], and is thus available for experimental efforts to assess the results of the computational study.

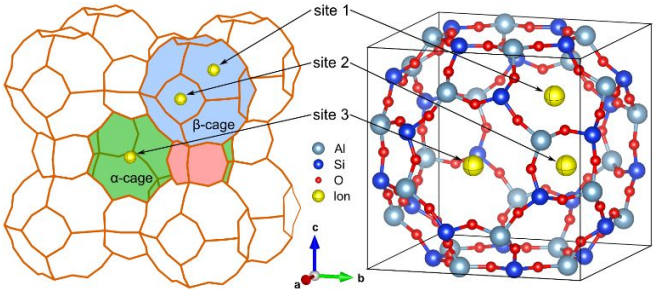


**Fig. 1** Left: schematic representation of LTA zeolite, with the *α*–cage, *β*–cage and double 4-member rings shown in green, blue and red, respectively. Right: Model of the *α*–cage, with the Al, Si, O and the adsorbed ions shown in cyan, blue, red and yellow, respectively.

We performed first-principles calculations using density functional theory (DFT), via the Vienna ab initio simulation package (VASP) plane-wave based code [26,27]. The generalized gradient approximation (GGA) of PBE [28] and projector augmented wave (PAW) potentials [29,30] were used to treat the exchange-correlation energy density functional and the ion-electron interactions, respectively. We also considered Van der Waals corrections, with dispersion interactions in the form of the DFT-D3 method[31]. The valence electronic configurations considered for construction of PAW potentials for Na, Ca, Sr, Ba, Si and O are $2p^6 3s^1$, $3p^6 4s^2$, $4s^2 4p^6 5s^2$, $5s^2 5p^6 6s^2$ and $3s^2 3p^2$ and $2s^2 2p^4$, respectively. A plane wave basis set with an energy cut-off of 520 eV was used to expand the electronic wave functions, with a $10^{-8}$ eV energy convergence criteria. For sampling the Brillouin zone, we used a 3×3×3 *k*-point mesh. The ground state geometries at 0 K were optimized by relaxing the cell volume and atomic positions until the maximum forces on each atom were less than 0.001 eV/Å, while keeping the cubic framework constant. To obtain a more accurate model of ion exchange in aqueous solutions, we considered the systems to be surrounded by water in addition to the usual simple vacuum environment, employing the implicit solvation model VASPsol[32,33].

For each of the studied ions and adsorption sites we calculated the ion adsorption energy, $E^{\mathrm{A}}_{\mathrm{ads},0}$, from

$$E^{\mathrm{A}}_{\mathrm{ads},0} = E(\mathrm{LTA{:}A}) - E(\mathrm{LTA}) - \mu^0_{\mathrm{A}}, \qquad (1)$$

where *E*(LTA:A) and *E*(LTA) are the DFT calculated total energies of the ps-LTA zeolite with and without adsorbed ion A, respectively. The standard chemical potential of ion A, $\mu^0_{\mathrm{A}}$ , is DFT calculated total energy of the single ion for the system in vacuum, while for the system in water it is set to be the scaled experimental standard chemical potential of the ion, as proposed by Persson et. al. [34]. The standard chemical potentials used in this study are given in Table S1. Varying the ion concentration in water requires $\mu^0_{\mathrm{A}}$ be replaced with the solution ion chemical potential, $\mu_{\mathrm{A}}$, defined as:

$$\mu_{\mathrm{A}} = \mu^0_{\mathrm{A}} + k_b T \ln(x_{\mathrm{A}}\gamma_{\mathrm{A}}), \qquad (2)$$

where $\mu_{\mathrm{A}}$, $x_{\mathrm{A}}$ and $\gamma_{\mathrm{A}}$ are the chemical potential, mole fraction and activity coefficient of ion A in water, respectively, $k_b$ is the Boltzmann constant and *T* is the thermodynamic temperature. The $\gamma_{\mathrm{A}}$ values were calculated using the Debye-Hückel equation, where the constants were found by fitting the reported experimental activity data of Kielland et. al. [35]. The resulting constants are given in Table S2. Introducing $\mu_{\mathrm{A}}$ allows the ion mole fraction at which ion $A_1$ becomes preferred over ion $A_2$ to be determined, which is found from the adsorption energy difference, $\Delta E_{\mathrm{ads}}$, defined as:

$$\Delta E_{\mathrm{ads}} = E^{\mathrm{A}_1}_{\mathrm{ads}} - E^{\mathrm{A}_2}_{\mathrm{ads}} = E^{\mathrm{A}_1}_{\mathrm{ads},0} - E^{\mathrm{A}_2}_{\mathrm{ads},0} - k_b T \ln\left(\frac{x_{\mathrm{A}_1}\gamma_{\mathrm{A}_1}}{x_{\mathrm{A}_2}\gamma_{\mathrm{A}_2}}\right). \qquad (3)$$

To predict the ability of ps-LTA's zeolite to exchange $Na^+$ ions for other ions of interest we need to determine the driving force for ion exchange, i.e., the ion exchange energy, $\Delta E^0_{\mathrm{ie}}$. The ion exchange reaction in zeolites can be described as:

$$\mathrm{A}_1(\mathrm{aq}) + \mathrm{A}_2(\mathrm{zeo}) = \mathrm{A}_1(\mathrm{zeo}) + \mathrm{A}_2(\mathrm{aq}) \qquad (4)$$

with the absorption energies described in Eq. (1) the ion exchange energy, $\Delta E^0_{\mathrm{ie}}$, can be defined as:

$$\Delta E^0_{\mathrm{ie}} = E^{\mathrm{A}_1}_{\mathrm{ads},0} - E^{\mathrm{A}_2}_{\mathrm{ads},0} = E(\mathrm{LTA{:}A_1}) - E(\mathrm{LTA{:}A_2}) - \mu^0_{\mathrm{A}_1} + \mu^0_{\mathrm{A}_2} \qquad (5)$$

Note that because of the different charge between the ions, our systems are also differently charged. In such a case the ion exchange energy, $\Delta E^{\mathrm{q}}_{\mathrm{ie}}$, should include the charge difference between ps-LTA zeolites with adsorbed $Na^+$ and $AE^{2+}$ ions. The $\Delta E^{\mathrm{q}}_{\mathrm{ie}}$ thus depends on the electron chemical potential, $\varepsilon_f$, i.e., the location of the Fermi level, as well as the charge difference between the systems, $\Delta q$, from

$$\Delta E^q_{\mathrm{ie}} = \Delta E^0_{\mathrm{ie}} + \Delta q \cdot \varepsilon_f = E^{\mathrm{A}_1}_{\mathrm{ads},0} - E^{\mathrm{A}_2}_{\mathrm{ads},0} + (q_1 - q_2)\varepsilon_f, \qquad (6)$$

where $\Delta q = 1$ as $q_1 = 2$ for AE and $q_2 = 1$ for Na. Similarly, the $\Delta q$ and $\varepsilon_f$ also influence the adsorption energy difference, $\Delta E^q_{\mathrm{ads}}$, following:

$$\Delta E^q_{\mathrm{ads}} == E^{\mathrm{A}_1}_{\mathrm{ads},0} - E^{\mathrm{A}_2}_{\mathrm{ads},0} - k_b T \ln\left(\frac{x_{\mathrm{A}_1}\gamma_{\mathrm{A}_1}}{x_{\mathrm{A}_2}\gamma_{\mathrm{A}_2}}\right) + (q_1 - q_2)\varepsilon_f. \qquad (7)$$

By defining the chemical potential of ions $A_1$ and $A_2$ at equilibrium, i.e., $\Delta E_{\mathrm{ie}} = 0$, the ion exchange isotherms for one to one exchange of $Na^+$ ion with AE ions can be determined at standard state, $T = 298$ K and $c_0 = 0.1$ M, as detailed in Kocevski at al.[24], using the equation:

$$X^{\mathrm{i}}_{A_1} = \frac{\sqrt{aX^{\mathrm{sol}}}}{1+\sqrt{aX^{\mathrm{sol}}}};\text{where}$$
$$X^{\mathrm{sol}} = \frac{X^{\mathrm{sol}}_{\mathrm{A}_1}}{1 - X^{\mathrm{sol}}_{\mathrm{A}_1}};\ a = e^{\frac{-\Delta E^0_{\mathrm{ie}}}{k_b T}} \frac{Q^i_{\mathrm{A}_1}\gamma_{\mathrm{A}_1}}{Q^i_{\mathrm{A}_2}\gamma_{\mathrm{A}_2}};\text{and } \Delta E^0_{\mathrm{ie}} = E^{\mathrm{A}_1}_{\mathrm{ads},0} - E^{\mathrm{A}_2}_{\mathrm{ads},0}, \qquad (8)$$

where $X^i_{A_1}$ and $X^{\mathrm{sol}}_{\mathrm{A}_1}$ are the mole fraction of ion $A_1$ on the *i* site of the zeolite and in solution, respectively, and $Q^i_{\mathrm{A}}$ is the partition function of the adsorbed ion A on site *i*. The ion-exchange isotherms as a function of the electron chemical potential can be calculated by replacing $\Delta E^0_{\mathrm{ie}}$ with $\Delta E^q_{\mathrm{ie}}$ in Eq. (8).

## Results and Discussion

### Ion Adsorption

Initial information on the interaction between the $AE^{2+}$ ions and ps-LTA zeolite were derived from the ion adsorption energies. Using Eq. (1) we calculated the adsorption energies, $E^{\mathrm{A}}_{\mathrm{ads},0}$, of $AE^{2+}$ ions and $Na^+$ at the three adsorption sites in ps-LTA zeolite in vacuum and water, using PBE and DFT-D3, respectively. The results are listed in Table 1. It is evident that the $E^{\mathrm{A}}_{\mathrm{ads},0}$ values calculated using DFT-D3 are always more negative compared to those calculated using PBE, which results from the stronger bonding from dispersion interactions in DFT-D3. Despite differences in the absolute values of $E^{\mathrm{A}}_{\mathrm{ads},0}$ calculated using PBE or DFT-D3 for sites 1 and 3, the energetic difference between

$Sr^{2+}$ or $Ba^{2+}$ and $Na^{+}$ are similar. On the other hand, for site 2 the differences calculated using DFT-D3 are less than those from PBE. The smaller size and larger charge of $AE^{2+}$ ions causes stronger bonding with adsorption site O atoms than for alkali ions [24], with the exception of $Na^{+}$, allowing the $AE^{2+}$ ions to bond at site 2. The ability to also adsorb ions on an additional site expands the ps-LTA capability to retain AE ions, increasing its possible utility in sequestering Sr and Ba radionuclides.

**Table 1** Adsorption energies, $E^{A}_{ads,0}$, in eV, of ions in vacuum, and water, at the three adsorption sites, calculated by PBE and DFT-D3.

| | | site 1 | | site 2 | | site 3 | |
|---|---|---|---|---|---|---|---|
| | ion | PBE | DFT-D3 | PBE | DFT-D3 | PBE | DFT-D3 |
| vacuum | $Na^{+}$ | -8.039 | -8.512 | -7.265 | -7.358 | -7.537 | -7.987 |
| | $Ca^{2+}$ | -22.178 | -22.167 | -20.824 | -20.952 | -21.462 | -21.721 |
| | $Sr^{2+}$ | -21.118 | -21.554 | -19.781 | -20.181 | -20.313 | -20.759 |
| | $Ba^{2+}$ | -19.548 | -20.650 | -18.211 | -19.681 | -18.743 | -20.259 |
| water | $Na^{+}$ | -1.643 | -2.026 | -1.414 | -1.480 | -1.432 | -1.793 |
| | $Ca^{2+}$ | -0.960 | -1.264 | -0.392 | -0.473 | -0.942 | -1.220 |
| | $Sr^{2+}$ | -1.710 | -2.097 | -1.333 | -1.624 | -1.439 | -1.731 |
| | $Ba^{2+}$ | -2.129 | -2.605 | -1.758 | -2.288 | -1.661 | -2.224 |

The most noticeable results in Table 1 are: i) the absorption energies $E^{A}_{ads,0}$ of $AE^{2+}$ ions in vacuum is much more negative than those in water, which can be explained by the more positive standard chemical potential of $AE^{2+}$ ions in vacuum as sown in Table S1; ii) the difference of absorption energy $E^{A}_{ads,0}$ for $Na^{+}$ and the $AE^{2+}$ ions in water is much smaller than that in vacuum because they have comparable chemical potentials in water; and iii) the negative absorption energy $E^{A}_{ads,0}$ of Na, Ca, Sr, and Ba ions at site 1, 2, and 3 in water increases in the order from Ca, Na, Sr and Ba ions which is different from that in vacuum. the $E^{A}_{ads,0}$ for $Ba^{2+}$ is more negative than for $Na^{+}$ for each of the three adsorption sites, with exchange among these ions highly favored. On the other hand, The $E^{A}_{ads,0}$ for $Ca^{2+}$ is always more positive than that of $Na^{+}$ at each of the adsorption sites (Table 1), thus an exchange between $Na^{+}$ in ps-LTA and $Ca^{2+}$ in water is not energetically favored. However, complete exchange of $Na^{+}$ with $Ca^{2+}$ in an LTA has been experimentally observed[36,37]. This discrepancy between the experiment and calculation may arise from using ps-LTA as a model system instead of the LTA zeolite, specifically neglecting the effect of replacing Si with Al as is the case in the zeolite.

The case for $Sr^{2+}$ ion is slightly more complex as $E^{A}_{ads,0}$ for $Sr^{2+}$ is more negative than for $Na^{+}$ on site 1, while for the other two sites the average value $E^{A}_{ads,0}$ of $Sr^{2+}$ and $Na^{+}$ calculated from PBE and DFT-D3 are similar. The results show that the exchange between $Na^{+}$ for $Sr^{2+}$ at site 1 in the ps-LTA zeolite is energetically favored. With $E^{A}_{ads,0}$ for $Ba^{2+}$ more negative than that for $Sr^{2+}$ also implies that $Ba^{2+}$ ions will be preferentially adsorbed. However, the adsorption energy of ions strongly depends on the chemical potential of ion in the medium which is a function of ion concentration and temperatures. Therefore, the chemical potentials of ions in the medium will dramatically affect the ion exchanges and equilibrium concentration of $AE^{2+}$, i.e., the capacity in LTA. The big difference between the adsorption energies calculated in vacuum and water reinforced our previous finding that a more accurate representation of ion-zeolite interaction requires consideration of the water environment [24]. While the greatest accuracy requires modeling water molecules and balancing anions, the required size of such a model exceeds current DFT capability.

**Ion Exchange**

The driving force for exchanging $Na^{+}$ with an $AE^{2+}$ ion can be analyzed from the dependence of the adsorption energy difference, $\Delta E_{ads}$, (Eq. 3), on the molar ratio of the ions, $x$(AE)/$x$(Na) in water, at 298 K. The ion exchange occurs if $\Delta E_{ads}$ is positive (as shown in Fig. S1). The $x$(AE)/$x$(Na) values at which $\Delta E_{ads}$ = 0 eV for all adsorption sites are listed in Table 2. It is found that a very high $Ca^{2+}$ concentration ($x(Ca^{2+})/x(Na) > 10^{7}$) is required to exchange $Na^{+}$ with $Ca^{2+}$ because of a more positive adsorption energy of $Ca^{2+}$compare to that of $Na^{+}$. The opposite is true for $Ba^{2+}$ exchange with $Na^{+}$ requiring only very low $Ba^{2+}$ concentrations ($x(Ba^{2+})/x(Na) < 10^{-5}$). In the case of $Sr^{2+}$, the $x$(AE)/$x$(Na) ratio at which $\Delta E_{ads}$ = 0 eV is ~$10^{\pm 2}$ for each of the three sites, such that small variations in concentration can drive $Na^{+}/Sr^{2+}$ ion exchange in either direction. Site 1 adsorption for $Sr^{2+}$ is favored until the $Na^{+}$ concentration is 23 times greater than that of $Sr^{2+}$. The results are less clear for site 2, where for $Sr^{2+}$ and $Ba^{2+}$ ions DFT-D3 computes lower $x$(AE)/$x$(Na) values as compared to site 1, and which also differ from PBE calculated values. The latter arises from the difference in values for $E^{A}_{ads,0}$ calculated using PBE and DFT-D3 for site 2.

The efficiency of $Sr^{2+}$/Na+ ion exchange can also be analyzed from $Sr^{2+}$ uptake point of view, considering a $Sr^{2+}$ solution that is passed through ps-LTA with a $Na^{+}$ normalized concentration of 1. In such case, the $Sr^{2+}$ concentration needs to be <0.042 for the ion exchange driving force to be zero, resulting in a 95.8 % $Sr^{2+}$ capacity in the ps-LTA. This value is in agreement with the 99.9 % $Sr^{2+}$ capacity measured in a LTA zeolite [20] and the 94 % capacity predicted in the phase-field modeling [25]. Given the lack of consideration of finite temperature in our calculations, namely the vibrational contribution to the energy, and/or from the use a simplified model of LTA, i.e., ps-LTA, these remain small differences in determined values.

**Table 2** x(AE)/x(Na) ratio at which the adsorption energy difference, $\Delta E_{ads}$ = 0 eV, at the three adsorption sites, calculated with PBE and DFT-D3. The $\Delta E_{ads}$ as a function of the x(AE)/x(Na) ratio is shown in Fig. S1.

| | site 1 | | site 2 | | site 3 | |
|---|---|---|---|---|---|---|
| ion | PBE | DFT-D3 | PBE | DFT-D3 | PBE | DFT-D3 |
| $Ca^{2+}$ | $8.79\cdot10^{10}$ | $1.86\cdot10^{12}$ | $4.13\cdot10^{16}$ | $2.34\cdot10^{16}$ | $4.86\cdot10^{7}$ | $1.19\cdot10^{9}$ |
| $Sr^{2+}$ | $4.50\cdot10^{-2}$ | $4.08\cdot10^{-2}$ | $1.47\cdot10^{1}$ | $2.48\cdot10^{-3}$ | $4.97\cdot10^{-1}$ | $6.69\cdot10^{0}$ |
| $Ba^{2+}$ | $4.15\cdot10^{-9}$ | $1.13\cdot10^{-10}$ | $1.02\cdot10^{-6}$ | $1.71\cdot10^{-14}$ | $8.70\cdot10^{-5}$ | $3.75\cdot10^{-8}$ |

The different charges of the systems cause the ion exchange energy, $\Delta E^{q}_{ie}$, to also depend on the electron chemical potential, $\varepsilon_f$., as discussed in Sec. II (Eq. 6). Shown in Table 3 is the $\varepsilon_f$ at which $\Delta E^{q}_{ie}$ = 0 eV for each of the sites, calculated using PBE and DFT-D3, and the dependence of $\Delta E^{q}_{ie}$ on $\varepsilon_f$ is shown in Fig. S2. Negative $\Delta E^{q}_{ie}$ values provide a thermodynamic driving force for exchanging the $Na^{+}$ with $AE^{2+}$. Evidently, change in the $\varepsilon_f$ does not influence $\Delta E^{q}_{ie}$ values of $Ca^{2+}$ at any of the 3 sites, due to the positive $\Delta E^{0}_{ie}$. A DFT-D3 calculated very small increase, ~0.07 eV, in $\varepsilon_f$ can prevent the exchange of $Na^{+}$ with $Sr^{2+}$ on site 1, as does a slightly larger $\varepsilon_f$, 0.14 eV, for site 2. In the case of $Ba^{2+}$, an increase of ~0.5 eV in $\varepsilon_f$ is needed to eliminate the thermodynamic driving force for ion exchange on site 1. Also, DFT-D3 for $Ba^{2+}$ ion computes larger $\varepsilon_f$ values as compared to PBE. Increasing $\varepsilon_f$ implies that electrons need to be donated to the ps-LTA, which is possible to control by doping the ps-LTA framework with an *n*-dopant, e.g., replacing Si with P or replacing O with F. It can also be

accomplished by introducing electron donors in the aqueous solution that interact with the ps-LTA framework, e.g., decreasing the pH. On the other hand, introducing *p*-dopants, such as Al, or increasing the pH of the aqueous solution would promote $AE^{2+}$ ion adsorption.

**Table 3** Electron chemical potential, $\varepsilon_f$ (in eV), at which the ion exchange energy, $\Delta E_{ie}^{q}$ = 0 eV, at the three adsorption sites, calculated with PBE and DFT-D3. The cells denoted with "n/a" indicate that at $\varepsilon_f$ = 0, $\Delta E_{ie}^{q}$ > 0 eV. $\Delta E_{ie}^{q}$ as a function of $\varepsilon_f$, is shown in Fig. S2.

| | site 1 | | site 2 | | site 3 | |
|---|---|---|---|---|---|---|
| ion | PBE | DFT-D3 | PBE | DFT-D3 | PBE | DFT-D3 |
| $Ca^{2+}$ | $8.79{\cdot}10^{10}$ | $1.86{\cdot}10^{12}$ | $4.13{\cdot}10^{16}$ | $2.34{\cdot}10^{16}$ | $4.86{\cdot}10^{7}$ | $1.19{\cdot}10^{9}$ |
| $Sr^{2+}$ | $4.50{\cdot}10^{-2}$ | $4.08{\cdot}10^{-2}$ | $1.47{\cdot}10^{1}$ | $2.48{\cdot}10^{-3}$ | $4.97{\cdot}10^{-1}$ | $6.69{\cdot}10^{0}$ |
| $Ba^{2+}$ | $4.15{\cdot}10^{-9}$ | $1.13{\cdot}10^{-10}$ | $1.02{\cdot}10^{-6}$ | $1.71{\cdot}10^{-14}$ | $8.70{\cdot}10^{-5}$ | $3.75{\cdot}10^{-8}$ |

## Isotherms

The ion exchange equilibrium can be further investigated by evaluating the ion exchange isotherms, as defined by Eq. (8) for $T$ = 298 K and $c_0$ = 0.1 M. Ion exchange isotherms for $Ca^{2+}$, $Sr^{2+}$ and $Ba^{2+}$ in water calculated using PBE and DFT-D3 are plotted in Fig. 2. The results show that $Ca^{2+}$ ion exchange is not possible at any of the adsorption sites, reflecting the high positive ion exchange energy values (Table S3). On the other hand, complete exchange of $Na^{+}$ for $Ba^{2+}$ is possible at all three adsorption sites, due to the large negative ion exchange energies calculated by either PBE or DFT-D3 (Table S3). In the case of $Sr^{2+}$, both PBE and DFT-D3 calculate only partial ion exchange is possible on the three adsorption sites. Unlike $Ca^{2+}$ and $Ba^{2+}$, the ion exchange energies for $Sr^{2+}$ have smaller and more similar values (Table S3), distributed around the 0 by ±0.07 eV, implying a possibility for only partial ion exchange. Having the possibility to completely or to a high extent exchange $Na^{+}$ for $Ba^{2+}$ or $Sr^{2+}$ is requirement for sequestering these radionuclides from nuclear wastewater using the ps-LTA zeolite.

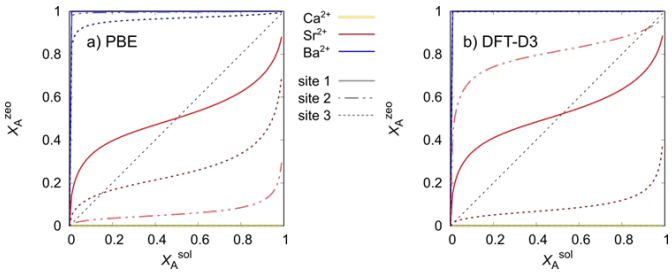


**Fig. 2** Ion exchange isotherms calculated using (a) PBE, and (b) DFT-D3 for ions on sites 1 (solid line), 2 (dashed-dotted line) and 3 (dashed line).

By replacing the $\Delta E_{ie}^{0}$ in Eq. (8) with $\Delta E_{ie}^{q}$, the ion exchange isotherms can also be plotted as a function of $\varepsilon_f$. Focusing only on site 1, the most probable adsorption site for $AE^{2+}$ and therefore that of greatest importance. Fig. 3 shows the ion exchange isotherms for $Sr^{2+}$ and $Ba^{2+}$ for a range of $\varepsilon_f$ values. From Fig. 3a and 3b it is clear that the ion exchange of $Na^{+}$ for $Sr^{2+}$ is no longer possible when $\varepsilon_f$ > 0.4 eV, when calculated with both PBE and DFT-D3. In the case of $Ba^{2+}$, partial exchange becomes dominant for $\varepsilon_f$ > 0.4 in PBE and for $\varepsilon_f$ > 0.5 eV in DFT-D3 calculations. Increasing in $\varepsilon_f$ further suppresses the $Ba^{2+}$ ion exchange, and not possible for $\varepsilon_f$ > 0.8 eV and for $\varepsilon_f$ > 0.9 eV in PBE and DFT-D3 calculations, respectively.

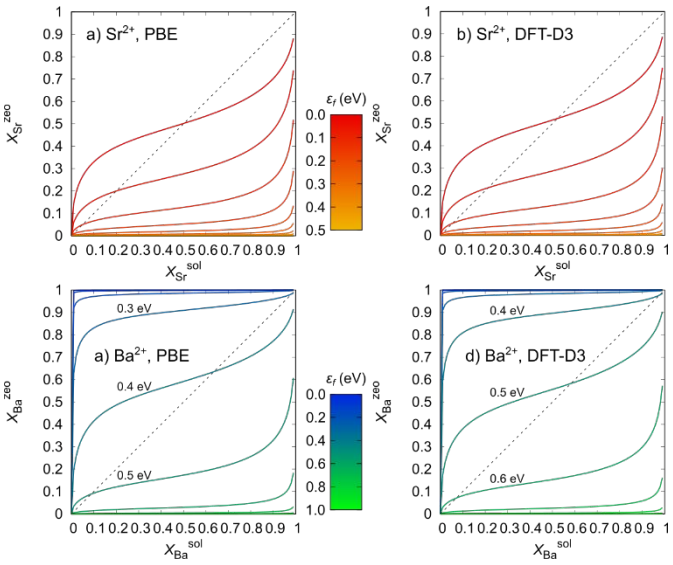


**Fig. 3** Ion exchange isotherms for various values of the electron chemical potential, $\varepsilon_f$, for $Sr^{2+}$ calculated using (a) PBE, and (b) DFT-D3, and $Ba^{2+}$ calculated using (c) PBE, and (d) DFT-D3. The color change from red to yellow and blue to green shows the increase in $\varepsilon_f$ for the systems containing $Sr^{2+}$ and $Ba^{2+}$, respectively.

The ion exchange between $Sr^{2+}$ and $Ba^{2+}$ ions shown in Fig. 4, indicate $\Delta E_{ads}$ is negative, and therefore existence of a thermodynamic driving force for exchanging $Ba^{2+}$ with $Sr^{2+}$ yielding ion exchange isotherms. Evidently, for ion exchange to be spontaneous, a very large $x$(Sr)/$x$(Ba) ratio is required (Fig. 4a), i.e., $10^{3}$ - $10^{11}$ depending on the site and potential used. The large $\Delta E_{ads}$ values influence the ion exchange isotherms, allowing only partial exchange on site 3 as calculated using PBE (Fig. 4b). This indicates that when using only a ps-LTA zeolite to capture $Ba^{2+}$ and $Sr^{2+}$, the protocol should require that $Ba^{2+}$ is removed first, with removal of $Sr^{2+}$ in a subsequent step. The larger $\Delta E_{ads}$ computed by DFT-D3 results from the stronger induced bonding between the larger $Ba^{2+}$ and the ps-LTA zeolite as compared to $Sr^{2+}$. This in turn decreases the $Ba^{2+}$ adsorption energy with respect to $Sr^{2+}$, increasing $\Delta E_{ads}$. Also, there is an evident trend with the $\Delta E_{ads}$ decreasing from site 3, to site 1 and to site 2, computed by either PBE or DFT-D3.

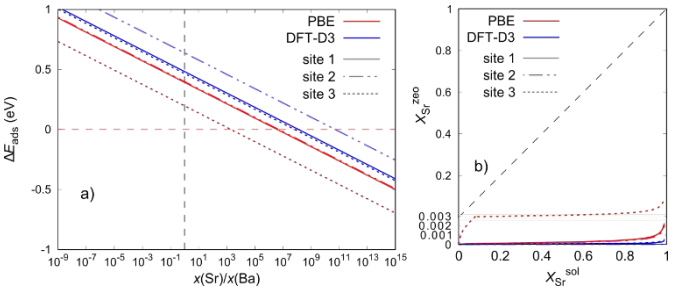


**Fig. 4** (a) adsorption energy difference, $\Delta E_{ads}$, and (b) ion exchange isotherms for exchanging $Ba^{2+}$ with $Sr^{2+}$ on site 1 (solid line), site 2 (dashed-dotted line) and site 3 (dashed line), calculated using PBE, and DFT-D3. The $\Delta E_{ads}$ and isotherms calculated using PBE and DFT-D3 are shown in red and blue, respectively.

## Conclusions

In vacuum, the adsorption energies of alkaline earth ions were significantly more negative than the energy of $Na^{+}$ adsorption. The difference in energies was substantially lessened, coming close to

zero, when the ions were solvated in water. We show that this discrepancy results from the large difference in the chemical potential of the alkaline earth ions and $Na^+$ in vacuum. This emphasizes that the solvation model is necessary for a more accurate representation of ion adsorption on zeolites. Moreover, we showed that $Na^+$ exchange with $Ba^{2+}$ is possible on all three adsorption sites as reflected by the large difference in $Na^+$ and $Ba^{2+}$ adsorption energies. On the other hand, $Ca^{2+}/Na^+$ ion exchange is not possible, unless the $x(Ca^{2+})/x(Na^+)$ ratio is considerably large ($> 10^7$), differently from the experiments. We argue that this discrepancy arises from using the ps-LTA as a model in our calculations. In the case of $Sr^{2+}$, the $Na^+$ ion exchange is only partially possible, with calculated normalized concentration of $Sr^{2+}$ in the zeolite of 0.9583. The calculated value is slightly lower than the experimentally observed one, which we argue is a result of not taking vibrational contributions to the energy into account when using ps-LTA as a computational model. The results demonstrate that ps-LTA can be successfully used for sequestering $Ba^{2+}$ and $Sr^{2+}$ radionuclides.

Furthermore, we showed that the ps-LTA electron chemical potential has a considerable influence on the ion exchange. This means that defects in the ps-LTA framework or the introduction of electron donors in the aqueous solution can suppress on the $Na^+$ ion exchange with alkaline earth ions. Also, we demonstrate that when using PBE calculations, exchanging $Ba^{2+}$ with $Sr^{2+}$ is only partially possible on site 3, but not on the remaining adsorption sites, while when considering DFT-D3, $Ba^{2+}/Sr^{2+}$ exchange was not possible on any of the adsorption sites. In aqueous solution, a very large $x(Sr^{2+})/x(Ba^{2+})$ ratio ($>10^7$) is required to overcome the $Ba^{2+}$ adsorption and for $Sr^{2+}$ to preferentially adsorb on the ps-LTA.

## Conflicts of interest

There are no conflicts to declare.

## Acknowledgements

This work is supported by the U.S. Department of Energy, Office of Science, Basic Energy Sciences, under Award No. DE-SC0016574 (Center for Hierarchical Waste Form Materials). This research used computational resources provided by the National Energy Research Scientific Computing Center (NERSC) and the HPC cluster Hyperion, supported by The Division of Information Technology at University of South Carolina.

## Notes and references

1. M. E. Davis, R. F. Lobo, *Chem. Mater.*, 1992**, 4**, 756.
2. A. Corma, *Chem. Rev.*, 1995**, 95**, 559.
3. A. Corma, *Chem. Rev.*, 1997**, 97**, 2373.
4. P. J. Davis, H. Bekkum, E. N. Coker, *J. Chem. Educ.*, 1999**, 76**, 469.
5. M. Kuronen, R. Harjula, J. Jernström, M. Vestenius, J. Lehto, *Phys. Chem. Chem. Phys.*, 2000, **2**, 2655.
6. C. R. Marcilly, *Top. Catal.*, 2000**, 13**, 357.
7. J. Weitkamp, *Solid State Ion.*, 2000**, 131**, 175.
8. D. M. Ruthven, S. C. Reyes, *Micropor. Mesopor. Mat.*, 2007, **104**, 59.
9. C. Perego, A. Bosetti, *Micropor. Mesopor. Mat.*, 2011, **144**, 28.
10. A. Feliczak-Guzik, *Micropor. Mesopor. Mat.*, 2018, **259**, 33.
11. A. Bhan, M. Tsapatsis, *Curr. Opin. Chem. Eng.*, 2013, **2**, 320.
12. M. Adabbo, D. Caputo, B. Gennaro, M. Pansini, C. Colella, *Micropor. Mesopor. Mat.*, 1999**, 28**, 315.
13. D. W. Breck, W. G. Eversole, R. M. Milton, T. B. Reed, T. L. Thomas, *J. Am. Chem. Soc.*, 1956, **78**, 5963.
14. R. P. Townsend, E. N. Coker, Chapter 11 Ion exchange in zeolites in: *Studies in Surface Science and Catalysis*, Elsevier, 2001, pp 467-524.
15. O. Cheung, N. Hedin, *RSC Adv.*, 2014, **4**, 14480.
16. E. I. Basaldella, P. G. Vázquez, F. Iucolano, D. Caputo, *J. Colloid Interface Sci.*, 2007, **313**, 574.
17. A. Malekpour, A. Samadi-Maybodi, M. R. Sadati, *Braz. J. Chem. Eng.*, 2011**, 28**, 669.
18. Y. P. Peña, W. Rondón, *Am. J. Analyt. Chem.*, 2013, **4**, 387.
19. H. Nakamura, M. Okumura, M. Machida, *J. Phys. Soc. Jpn.*, 2013, **82**, 023801.
20. M. W. Munthali, E. Johan, H. Aono, N. Matsue, *J. Asian Ceram. Soc.*, 2015, **3**, 245.
21. B. Said, A. Grandjean, Y. Barre, F. Tancret, F. Fajula, A. Galarneau, *Micropor. Mesopor. Mat.*, 2016, **232**, 39.
22. R. E. Salmas, B. Demir, E. Yıldırım, A. Sirkecioğlu, M. Yurtsever, M. G. Ahunbay, *J. Phys. Chem. C*, 2013, **117**, 1663.
23. C. E. Hernandez-Tamargo, A. Roldan, P. E. Ngoepe, N. H. Leeuw, *J. Chem. Phys.*, 2017, **147**, 074701.
24. V. Kocevski, B. D. Zeidman, C. H. Henager, T. M. Besmann, *J. Chem. Phys.*, 2018**, 149**, 131102.
25. Y. L. Li, B. D. Zeidman, S. Y. Hu, C. H. Henager, T. M. Besmann, A. Grandjean, *Comput. Mater. Sci.*, 2019**, 159**, 103.
26. G. Kresse , J. Furthmüller, *Comput. Mater. Sci.* **1996,** *6,* 15-50.
27. G. Kresse, J. Furthmüller, *Phys. Rev. B*, 1996, **54**, 11169.
28. J. P. Perdew, K. Burke, M. Ernzerhof, *Phys. Rev. Lett.*, 1997**, 78**, 1396.
29. P. E. Blöchl, *Phys. Rev. B*, 1994**, 50**, 17953.
30. G. Kresse, D. Joubert, *Phys. Rev. B*, 1999**, 59**, 1758.
31. S. Grimme, J. Antony, S. Ehrlich, H. Krieg, *J. Chem. Phys.*, 2010**, 132**, 154104.
32. M. Fishman, H. L. Zhuang, k. Mathew, W. Dirschka, R. G. Hennig, *Phys. Rev. B*, 2013**, 87**, 245402.
33. K. Mathew, R. Sundararaman, K. Letchworth-Weaver, T.A. Arias, R. G. Hennig, *J. Chem. Phys.*, 2014**, 140**, 084106.
34. K. A. Persson, B. Waldwick, P. Lazic, G. Ceder, *Phys. Rev. B*, 2012**, 85**, 235438.
35. J. Kielland, *J. Am. Chem. Soc.*, 1937**, 59**, 1675.
36. K. M. Abd El-Rahman, A. M. El-Kamash, M. R. El-Sourougy, N. M. Abdel-Moniem, *J. Radioanal. Nucl. Chem.,* 2006, **268**, 221.
37. A. Merceille, E. Weinzaepfel, Y. Barré, A. Grandjean, *Sep. Purif. Technol.*, 2012, **96**, 81.